The development of an industrial-scale fed-batch fermentation simulation

Article *in* Journal of Biotechnology · November 2014

DOI: 10.1016/j.jbiotec.2014.10.029

5 authors, including:

Stephen Goldrick
University College London
37 PUBLICATIONS **484** CITATIONS
SEE PROFILE

David Lovett
Perceptive Engineering
23 PUBLICATIONS **482** CITATIONS
SEE PROFILE

Gary Montague
Teesside University
238 PUBLICATIONS **4,088** CITATIONS
SEE PROFILE

Barry Lennox
The University of Manchester
276 PUBLICATIONS **5,358** CITATIONS
SEE PROFILE

Journal of Biotechnology 193 (2015) 70–82

Contents lists available at ScienceDirect

Journal of Biotechnology

journal homepage: www.elsevier.com/locate/jbiotec

The development of an industrial-scale fed-batch fermentation simulation

Stephen Goldrick[a,b,c], Andrei Ştefan[b], David Lovett[c], Gary Montague[a,1], Barry Lennox[b,*]

[a] Biopharmaceutical Bioprocess Technology Centre, Merz Court, Newcastle University, Newcastle-upon-Tyne, United Kingdom
[b] Control Systems Group, School of Electrical and Electronic Engineering, University of Manchester, Manchester, United Kingdom
[c] Perceptive Engineering Limited, Vanguard House, Keckwick Lane, Daresbury, Cheshire, United Kingdom

ARTICLE INFO

Article history:
Received 3 July 2014
Received in revised form 13 October 2014
Accepted 23 October 2014
Available online 1 November 2014

Keywords:
Industrial fermentation
Kinetic modelling
Penicillin production
Structured model
Simulation

ABSTRACT

This paper describes a simulation of an industrial-scale fed-batch fermentation that can be used as a benchmark in process systems analysis and control studies. The simulation was developed using a mechanistic model and validated using historical data collected from an industrial-scale penicillin fermentation process. Each batch was carried out in a 100,000 L bioreactor that used an industrial strain of *Penicillium chrysogenum*. The manipulated variables recorded during each batch were used as inputs to the simulator and the predicted outputs were then compared with the on-line and off-line measurements recorded in the real process. The simulator adapted a previously published structured model to describe the penicillin fermentation and extended it to include the main environmental effects of dissolved oxygen, viscosity, temperature, pH and dissolved carbon dioxide. In addition the effects of nitrogen and phenylacetic acid concentrations on the biomass and penicillin production rates were also included. The simulated model predictions of all the on-line and off-line process measurements, including the off-gas analysis, were in good agreement with the batch records. The simulator and industrial process data are available to download at www.industrialpenicillinsimulation.com and can be used to evaluate, study and improve on the current control strategy implemented on this facility.

1. Introduction

Industrial-scale production of antibiotics was pioneered through the development of deep tank fermentation during the scaling up of penicillin in the 1940s (Shuler and Kargi, 2002). This technique transformed the biotechnology sector into a billion dollar industry with deep-tank fermentations at its core. Despite the reliance of major pharmaceutical and biotech companies on large-scale fermentations, regulatory restrictions have limited innovation and decreased R&D into advanced process control strategies, which includes the development of mathematical models at this scale (Grabowski et al., 1978; Yu, 2008).

The majority of the research conducted on fermentation processes has used laboratory-scale equipment, some of this research has focused on developing first principle mathematical models. As penicillin was the first antibiotic to be commercially scaled up, a considerable amount of research has focused on quantitatively describing this process. Models defined for this type of process, range from highly complex structured models that consider the internal structure of the *Penicillium chrysogenum* fungus (Paul and Thomas, 1996; Megee et al., 1970; Nestaas and Wang, 1983; Nielsen, 1993), to more simplistic unstructured models based on kinetic expressions of growth profiles of penicillin and biomass (Righelato et al., 1968; Birol et al., 2002; Bajpai and Reul, 1980). Over the last decade it has been the simpler unstructured models which have been applied more frequently to industrial applications (Menezes and Alves, 1994). The most notable unstructured model is that developed by Bajpai and Reul (1980) which has been extended by Birol et al. (2002) and used as the standard test bed for almost every aspect of bioprocess control including multivariate statistical process monitoring and control (Lee et al., 2004; Ündey and Ertunç, 2003), regression model analysis (Zhang and Lennox, 2004) and optimisation of feeding strategies (Ashoori et al., 2009). However, based on the limited application of models in industry, there is a clear division between a useful academic fermentation model and a practical industrial one. It has been highlighted by Patnaik (2001) that the more information a model contains the more complex it becomes, which reduces its "usefulness" for monitoring and control

* Corresponding author. Tel.: +44 161 306 4661.
E-mail address: barry.lennox@manchester.ac.uk (B. Lennox).
[1] Current address: Teesside University, Middlesbrough, Tees Valley, United Kingdom.

http://dx.doi.org/10.1016/j.jbiotec.2014.10.029
0168-1656/

studies. However considering that simple unstructured models are not sufficient to capture complex process dynamics, structured models need to be utilised and applied to industrial processes to facilitate the development of enhanced control strategies.

The purpose of this research is to develop a realistic simulation of an industrial fermentation to be used as a benchmark in process control and optimisation studies. The work describes an extension of the structured penicillin fermentation model developed by Paul and Thomas (1996) and describes all the component balances relating to the process variables. The simulation was subsequently validated using the batch records from ten 100,000 L fed-batch penicillin fermentations. The simulator improves on previous fed-batch simulations as it considers the typical problems encountered on large-scale fermentations, including challenges associated with the control of the dissolved oxygen during highly viscous fermentations and controlling key nutrients using delayed off-line measurements. The simulator and industrial process data are available to download at www.industrialpenicillinsimulation.com. The simulator can also be used as a stand alone application which includes batch to batch variation, deviations relating to input concentrations and typical process faults including foaming, agitator tripping and problems relating to inaccurate sensors. The developed simulator provides a challenge for researchers to develop robust monitoring and control strategies applicable to a complex industrial-scale penicillin fermentation simulation.

2. Industrial-scale penicillin model

The structured model developed by Paul and Thomas (1996) was adapted and implemented here, as it has been shown to best describe the fermentation behaviour when compared with ten other penicillin models (Syndall, 1998). The simulation considers the growth, morphology, metabolic production and degeneration of the biomass during a submerged *P. chrysogenum* fermentation. The simulation divides the internal structure of the biomass or hyphae into four separate regions: actively growing regions (A_0), non-growing regions (A_1), degenerated regions (A_3) formed through vacuolation and autolysed regions (A_4), as illustrated in Fig. 1. This paper omits the description of the formation of vacuoles, which represent nutrient depleted regions of the hyphae whose growth is responsible for the formation of the degenerated regions (A_3). The vacuoles are defined by Paul and Thomas (1996) as vacuole regions (A_2). Paul and Thomas (1996) provide a full description of the formation and growth of these individual regions.

A component balance on the fermenter was performed and presented here. The parameters relating to the simulation presented are available in Table 1 and Table 2 and the parameters relating to the structured penicillin model are available in Table 1A.

Growing regions (A_0):

$$\frac{dA_0}{dt} = \underbrace{r_b}_{\text{branching}} - \underbrace{r_{diff}}_{\text{differentiation}} - \underbrace{\frac{F_{in}A_0}{V}}_{\text{dilution}} \quad (1)$$

Non-growing regions (A_1):

$$\frac{dA_1}{dt} = \underbrace{r_e}_{\text{extension}} - \underbrace{r_b}_{\text{branching}} + \underbrace{r_{diff}}_{\text{differentiation}} - \underbrace{r_{deg}}_{\text{degeneration}} - \underbrace{\frac{F_{in}A_1}{V}}_{\text{dilution}} \quad (2)$$

Degenerated regions (A_3):

$$\frac{dA_3}{dt} = \underbrace{r_{deg}}_{\text{degeneration}} - \underbrace{r_a}_{\text{autolysis}} - \underbrace{\frac{F_{in}A_3}{V}}_{\text{dilution}} \quad (3)$$

Table 1
Summary of model parameters.

Parameter	Description	Units
t	Batch time	h
A_0	Growing biomass concentration	g L^{-1}
A_1	Non-growing biomass concentration	g L^{-1}
A_3	Degenerated biomass concentration	g L^{-1}
A_4	Autolysed biomass concentration	g L^{-1}
X	Total biomass concentration	g L^{-1}
P	Penicillin concentration	g L^{-1}
s	Substrate concentration	g L^{-1}
V	Vessel Volume	L
V_m	Vessel Volume	m^3
F_{in}	Total flow in	L h^{-1}
F_{dis}	Discharge rate	L h^{-1}
F_s	Sugar flow rate	L h^{-1}
F_{PAA}	Phenylacetic acid flow	L h^{-1}
F_{oil}	Soybean oil flow rate	L h^{-1}
F_w	Water for injection flow rate	L h^{-1}
$F_{a/b}$	Acid/base flow rate	L h^{-1}
F_{evp}	Evaporation flow rate	L h^{-1}
DO_2	Dissolved oxygen concentration	mg L^{-1}
k_La	Volumetric mass transfer coefficient	h^{-1}
μ_{app}	Apparent viscosity	cP
F_g	Aeration rate	m^3 min^{-1}
P_{ag}	Agitator power	kW
P_{air}	Power dissipated by aeration	kW
P_1	Vessel back pressure	Pa
ρ_b	Density of broth	kg m^{-3}
P_0	Vessel bottom pressure	Pa
Z	Ungassed liquid height	m
T_b	Temperature of broth	K
H^+	Hydrogen ion concentration	mol L^{-1}
N_{shots}	Nitrogen shots	kg
PAA	Phenylacetic acid concentration	mg L^{-1}
N	Nitrogen concentration	mg L^{-1}
$O_{2_{out}}$	Oxygen off-gas concentration	%
$CO_{2_{out}}$	Carbon dioxide off-gas concentration	%
$CO_{2,L}$	Dissolved carbon dioxide concentration	g L^{-1}

Autolysed regions (A_4):

$$\frac{dA_4}{dt} = \underbrace{r_a}_{\text{autolysis}} - \underbrace{\frac{F_{in}A_4}{V}}_{\text{dilution}} \quad (4)$$

Total biomass (X):

$$X = A_0 + A_1 + A_3 + A_4 \quad (5)$$

Product formation (P):

$$\frac{dP}{dt} = \underbrace{r_P}_{\text{Production}} - \underbrace{r_h}_{\text{hydrolysis}} - \underbrace{\frac{F_{in}P}{V}}_{\text{dilution}} \quad (6)$$

Substrate consumption (s):

$$\frac{ds}{dt} = -\underbrace{Y_{s/X}r_e}_{\text{extension}} - \underbrace{Y_{s/X}r_b}_{\text{branching}} - \underbrace{m_s r_m}_{\text{maintenace}} - \underbrace{Y_{s/P}r_P}_{\text{production}} + \underbrace{\frac{F_s c_s}{V} + \frac{F_{oil}c_{oil}}{V}}_{\text{feedin}} - \underbrace{\frac{F_{in}s}{V}}_{\text{dilution}} \quad (7)$$

where, $r_{b,diff,e,deg,a,P,h,m}$ is the rate of branching, differentiation, extension, degeneration, autolysis, product formation, product hydrolysis and maintenance, respectively. The batch time is represented by t. $Y_{s/X}$ and $Y_{s/P}$ represents the substrate yield coefficients of biomass and penicillin, respectively, and m_s is the substrate maintenance term. F_s, F_{oil}, c_s and c_{oil} represents the sugar and soybean oil feed rate and concentrations, respectively. For simplicity the addition of oil was combined with sugar to form a representative single substrate, s. F_{in} represents all the process inputs

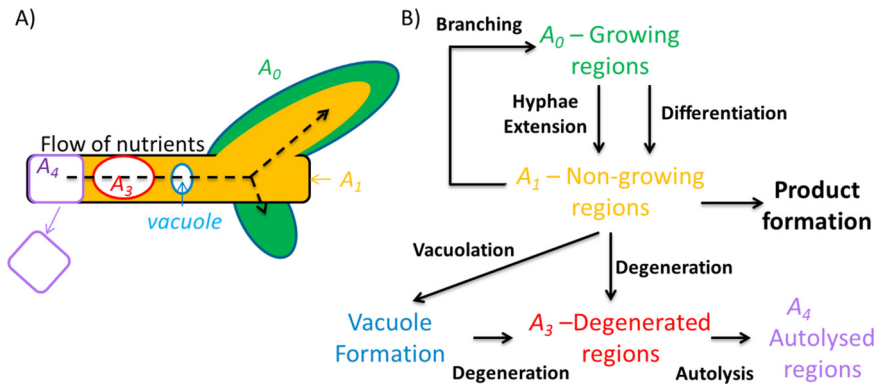

Fig. 1. (A) Schematic diagram illustrating the four separate regions of the *Penicillin chrysogenum* fungus with the flow of nutrients highlighted. (B) Mechanisms of formation for each region. Modified from Paul and Thomas (1996).

(excluding F_{dis}). The fermenter volume (V) change which is specific to the case study presented later is described as:

$$\frac{dV}{dt} = F_s + F_{oil} + F_{PAA} + F_a + F_b + F_w - F_{evp} - F_{dis} \quad (8)$$

where F_{PAA} is the flow rate of the phenylacetic acid and F_a and F_b are the flow rates of the acid and base, respectively. F_w is the flow rate of the water for injection which is typically used to reduce the broth viscosity. F_{evp} is the evaporation rate of the fermenter and F_{dis} is the volume discharged from the vessel during production to maintain the volume within its maximum working capacity.

Modifications to the simulation relate to the rate of differentiation (r_{diff}) of actively growing regions (A_0) to non-growing regions (A_1), which was original proposed by Megee et al. (1970) and described in Paul and Thomas (1996) as:

$$r_{diff} = \frac{\mu_{diff} A_0}{K_{diff} + s} \quad (9)$$

where μ_{diff} is the specific rate of differentiation, s is the substrate concentration, A_0 is the concentration of growing regions and K_{diff} is the differentiation saturation constant. Eq. (9) implies the transition of A_0 to A_1 is inhibited by substrate but can be assumed linear at very low substrate concentrations e.g. during the production phase. This proposed mechanism utilises a large proportion of the substrate incorporated through the substrate maintenance term in Eq. (7). This reduces the substrate available for growth and production, particularly during the initial stages of the batch. An improved prediction was obtained by defining the rate of differentiation to be proportional to the mean cell culture age (A_t) as defined in Tiller et al. (1994). This was modelled by describing the saturation constant for differentiation as a time dependant term:

$$K_{diff} = \begin{cases} 0.75 - \beta_1 A_t & K_{diff} > 0.09 \\ 0.09 & K_{diff} <= 0.09 \end{cases} \quad (10)$$

where K_{diff} is the saturation constant and β_1 is a constant. This modification implies that the specific rate of differentiation is negligible during the initial stages of the batch but becomes more influential with batch progression, up until it reaches its minimum value defined here as 0.09. The second adjustment that was made to the model assumes a Gaussian distribution for the substrate inhibition effect on the penicillin production rate (μ_p), defined as:

$$\mu_P = 2.5\mu_{P_{max}}\sigma_P \left(\frac{e^{-\frac{1}{2}\left(\frac{s - s\max_P}{\sigma_P}\right)^2}}{\sigma_P\sqrt{2\pi}} \right) \quad (11)$$

where σ_P relates to the substrate concentration range at which penicillin production will occur with the optimum production occurring at a substrate concentration defined by $s_{\max_P}$. This inhibition curve allows for the maximum theoretical specific production rate of penicillin ($\mu_{P_{max}}$) to be reached, in contrast to the inhibition curve proposed in Paul and Thomas (1996), which allows for 70% of the theoretical maximum to be obtained.

In addition to the described penicillin model, the following component balances were included in the simulation. The values of all the parameters defined in the following sections are provided in Tables 1 and 2.

2.1. Dissolved oxygen

Dissolved oxygen (DO_2) is a key macro-nutrient used by the micro-organism for growth, maintenance and metabolic production and was modelled by Bajpai and Reul (1980) as:

$$\frac{dDO_2}{dt} = -\mu_X X Y_{O_2/X} - \mu_P P Y_{O_2/P} - m_{O_2} X + k_L a(DO_2^* - DO_2) - \frac{DO_2 dV}{V dt} \quad (12)$$

The first three terms represent the oxygen uptake rate (OUR) which accounts for oxygen being consumed during biomass growth ($\mu_X X$), maintenance ($m_{O_2} X$), and penicillin production ($\mu_P P$). $Y_{O_2/X}$ and $Y_{O_2/P}$ are the oxygen yield coefficients for biomass and penicillin, respectively. μ_X represents the rate of change of the growing, non-growing, degenerated and autolysed regions. Oxygen transfer rate is the product of the volumetric mass transfer coefficient ($k_L a$) and the difference between the dissolved oxygen concentration (DO_2) and the oxygen saturation concentration (DO_2^*). $k_L a$ is modified from Garcia-Ochoa and Gomez (2009) to account for the effect of soybean oil and is defined as:

$$k_L a = \alpha_{k_L a} V_s^a \left(\frac{P_w}{V_m}\right)^b \mu_{app}^c \left(1 - \left(\frac{F_{oil}}{V}\right)^d\right) \quad (13)$$

where $\alpha_{k_L a}$ is a constant based on the geometrical parameters of the vessel and the stirrer employed and V_s is the superficial gas velocity taken as $F_g/\pi r^2$, with F_g as the volumetric flow rate of air and r as the tank radius. The exponents (a, b, and c) are empirical values, shown to be in the range of $0.4 \le a \le 1$, $0.3 \le b \le 0.7$ and $-0.4 \le c \le -0.7$ by Garcia-Ochoa and Gomez (2009). The exponent d was taken as 0.25 to account for the observed decrease in $k_L a$ as the flow rate of soybean oil was increased as highlighted in the case study discussed later. Similar findings were reported by Chern et al. (2001), who found a decrease in $k_L a$ with the addition of soybean oil in a 500 L tank. This $k_L a$ term accounts for the well known effects of oils and antifoam agents on the mass transfer of oxygen in bioreactors (Junker, 2007; Kawase and Moo-Young, 1990;

Table 2
Summary of simulation parameters

Parameter	Value (units)	Reference
Biomass substrate yield coefficient ($Y_{s/X}$)	1.85 g g^{-1}	Paul et al. (1998)
Penicillin substrate yield coefficient ($Y_{s/P}$)	0.9 g g^{-1}	Bajpai and Reul (1980)
Substrate maintenance term (m_s)	0.029 g g^{-1} h^{-1}	Paul and Thomas (1996)
Oil feed concentration (c_{oil})	1000 g L^{-1}	Estimated from industrial case study
Sugar feed concentration (c_s)	600 g L^{-1}	Estimated from industrial case study
Biomass oxygen yield coefficient ($Y_{O_2/X}$)	650 mg O_2 (g X)$^{-1}$	Christensen et al. (1995)
Penicillin oxygen yield coefficient ($Y_{O_2/P}$)	160 mg O_2 (g X)$^{-1}$	Bajpai and Reul (1980)
Maintenance oxygen coefficient (m_{O_2})	17.5 mg O_2 (g X)$^{-1}$	Modified from Christensen et al. (1995)
$k_l a$ constants, ($\alpha_{k_l a}$)	85 ± 14	Estimated from industrial case study
$k_l a$ constants, (a, b, c, d)	0.38, 0.34, −0.38, 0.25	Estimated from industrial case study
Henry's law constant (H_{O_2})	0.0251 bar L mg^{-1}	Green and Perry (2008)
Number of impellers (n)	3	Shuler and Kargi (2002)
Tank radius (r)	2.1 m	Shuler and Kargi (2002)
Impeller radius (r_{imp})	0.85 m	Shuler and Kargi (2002)
Gassed to ungassed power ration($P_g/P_{ungassed}$)	0.4–0.6	Estimated from industrial case study
Power number (Po)	5	Uhl and Gray (1966)
RPM (N_{RPM})	100	Estimated from industrial case study
Gas hold up (ϵ)	0.1	Estimated from industrial case study
Gravitational constant (g)	9.81 m s^{-2}	Green and Perry (2008)
Universal gas constant (R)	8.314 J K^{-1} mol^{-1}	Green and Perry (2008)
Penicillin critical dissolved oxygen level ($DO_{2_{crit_P}}$)	30%	Vardar and Lilly (1982)
Biomass critical dissolved oxygen level ($DO_{2_{crit_X}}$)	10%	Vardar and Lilly (1982)
Inhibition constant (A_{inhib})	1	Estimated from industrial case study
Temperature substrate and cold water (T_s, T_w)	288 K	Estimated from industrial case study
Temperature of hot water (T_h)	333 K	Estimated from industrial case study
Temperature of air (T_{air})	290 K	Estimated from industrial case study
Specific heat capacity substrate (C_{P_s})	5.8 kJ (kg K)$^{-1}$	Green and Perry (2008)
Specific heat capacity water and broth (C_{P_w}, C_{P_b})	4.18 kJ (kg K)$^{-1}$	Green and Perry (2008)
Heat evaporation ($\Delta_{H_{evp}}$)	2430.7 kJ kg^{-1}	Green and Perry (2008)
Vessel wall heat transfer coefficient (U_{jacket})	36 kW m^2	Estimated from Industrial case study
Area of cooling coils (A_c)	105 m^2	Vogel and Todaro (1997)
Arrhenius constant for cell growth (k_g)	450 J g X	Modified from Birol et al. (2002)
Arrhenius constant for cell death (k_d)	0.25×10^{30} J g X	Estimated from industrial case study
Activation energy for cell growth (E_g)	1.5×10^4 J mol^{-1}	Estimated from industrial case study
Activation energy for cell death (E_d)	1.75×10^5 J mol^{-1}	Estimated from industrial case study
Heat yield coefficients, biomass and penicillin ($Y_{Q/X}$, $Y_{Q/X}$)	25 kJ g^{-1}	Estimated from industrial case study
Acid/base inlet concentration (abc)	0.033 mol L^{-1}	Estimated from industrial case study
Hydrogen ion production term (γ_1)	3.25×10^{-3}	Estimated from industrial case study
Hydrogen ion process inputs term (γ_2)	2.5×10^{-11}	Estimated from industrial case study
Hydrogen ion maintenance term (m_{pH})	0.0025	Estimated from industrial case study
Hydrogen ion inhibition terms (K_1/K_2)	1×10^{-5}/ 2.5×10^{-8} mol L^{-1}	Estimated from industrial case study
Nitrogen concentration in oil feed ($c_{N_{oil}}$)	20 g L^{-1}	Estimated from industrial case study
Nitrogen concentration in *PAA* feed ($c_{N_{PAA}}$)	80 ± 28 g L^{-1}	Estimated from industrial case study
Nitrogen shots ($c_{N_{shot}}$)	400 g kg^{-1}	Estimated from industrial case study
N, Penicillin yield coefficient ($Y_{N/P}$)	80 mg g^{-1}	Estimated from industrial case study
N, Biomass yield coefficient ($Y_{N/X}$)	10 mg g^{-1}	Estimated from industrial case study
Maintenance *N* term, (m_N)	0.03 mg g^{-1} hr^{-1}	Estimated from industrial case study
Critical *N* concentration for biomass (N_{crit_X})	150 mg L^{-1}	Estimated from industrial case study
PAA feed solution concentration (c_{PAA})	530 ± 35 g L^{-1}	Estimated from industrial case study
PAA, Biomass yield coefficient ($Y_{PAA/X}$)	37.5 mg g^{-1}	Estimated from industrial case study
PAA, Penicillin yield coefficient ($Y_{PAA/P}$)	187.5 mg g^{-1}	Estimated from industrial case study
Maintenance *PAA* term, (m_{PAA})	1.2 mg g^{-1} h^{-1}	Estimated from industrial case study
Critical *PAA* concentration for biomass (PAA_{crit_X})	2000 mg L^{-1}	Estimated from industrial case study
Critical *PAA* concentration for penicillin (PAA_{crit_P})	200 mg L^{-1}	Estimated from industrial case study
Penicillin hydrolysis constants (B_1, B_2)	−67.8, −1.82	Kheirolomoom et al. (1999)
Penicillin hydrolysis constants (B_3, B_4, B_5)	0.36, 0.12, -4.9×10^{-4}	Kheirolomoom et al. (1999)
Volumetric mass transfer ratio ($\delta_{c/o}$)	0.89	Royce (1992)
Constant related to filamentous break up (k_{water})	0.005	Estimated from the Industrial case study
Viscosity coefficients (k_{in}, k_{de})	0.001, 0.0001	Estimated from the Industrial case study
Viscosity coefficients (t_{in}, t_{de})	1, 250 h	Estimated from the Industrial case study
Penicillin oxygen yield coefficient ($Y_{CO_2/X}$)	850 mg CO_2 (g X)$^{-1}$	Christensen et al. (1995)
Maintenance carbon dioxide coefficient (m_{CO_2})	66 mg CO_2 (g X)$^{-1}$ h^{-1}	Modified from Christensen et al. (1995)
Critical CO_2 concentration for biomass $CO_{2.L_{crit_X}}$)	35 mg L^{-1}	Estimated from industrial case study

Routledge, 2012). The oxygen saturation concentration (DO_2^*), was calculated using Henry's law as follows:

$$DO_2^* = \frac{O_{2,in} P_{lm}}{H_{O_2}} \tag{14}$$

where $O_{2,in}$ is the oxygen concentration in the air entering the vessel, P_{lm} is the log mean pressure of the vessel and H_{O_2} is Henry's equilibrium constant, obtained from Scragg (1991). The total power consumption (P_w) was taken as the sum of the power required for both agitation (P_{ag}), taken from Albaek et al. (2012), and aeration (P_{air}), taken from Roels and Heijnen (1980):

$$P_{ag} = \frac{n \mathrm{Po} \rho_b N_{rpm}^3 D^5 P_{ag}/P_{ungassed}}{1000} \tag{15}$$

where n is the number of impellers, Po the unaerated impeller power number approximated as 5 from Uhl and Gray (1966) assuming turbulent conditions in the vessel using Ruston impellers. N_{rpm} is the rpm and D the diameter of the impeller. The broth

density was modelled dynamically which considered the density of the media and the concentrations of both biomass and penicillin taken as $\rho_b = 1100 + X + P$. The relative power draw ($P_{ag}/P_{ungassed}$) is calculated from Scragg (1991) as the ratio of the gassed power consumption (P_{ag}) to the ungassed power consumption ($P_{ungassed}$) which is a function of the aeration rate, found to range from 0.4 to 0.6. The aeration power requirements are calculated as:

$$P_{air} = \frac{V_s R T_b V_m}{22.4Z} \ln\left(1 + \frac{\rho_b g Z}{P_0}\right) \quad (16)$$

where R is the universal gas constant, T_b the vessel temperature, g the gravitational constant and P_0 the pressure at the bottom of the vessel, calculated as:

$$P_0 = P_1 + \rho_b g(1-\varepsilon)Z \quad (17)$$

with P_1 is the vessel back pressure, Z the ungassed liquid height and ε the gas hold-up coefficient, assumed to be constant.

Control of the DO_2 concentration is paramount for aerobic fermentations and provided it is kept above a critical concentration ($DO_{2_{crit}}$) all microbial activities can be assumed to be unaffected (Finn, 1954). However, DO_2 concentrations below this critical limit result in a sharp decrease in biomass growth and metabolic production and unless this is quickly rectified, batch failure is generally imminent. The critical values of oxygen inhibition on cell growth and metabolic production in penicillin fermentations was investigated by Vardar and Lilly (1982) and found to be two distinct values. They observed that below 30% air saturation the specific growth rate of penicillin decreased sharply and below 10% air saturation penicillin production was impaired irreversibly, similar results were reported by Rolinson (1952). In order to take account of this physical phenomena, the simulation relates the specific growth rate of biomass and penicillin to the DO_2 concentration using a hyperbolic tangent function. For penicillin production (μ_P), this relationship assumes that provided the DO_2 concentration is above its critical value of 30% air saturation (taken from Vardar and Lilly (1982)), μ_P will be unaffected. However if the DO_2 drops below this value, μ_P will effectively go to zero. This relationship was modelled using a hyperbolic tangent function ranging from 0 to 1, described here as:

$$\mu_P \approx 0.5\mu_P(1 - \tanh(A_{inhib}(DO_{2_{crit_P}} - DO_2))) \quad (18)$$

where $DO_{2_{crit_P}}$ is the critical DO_2 concentration and A_{inhib} is a constant relating to the steepness of the transition of $\mu_P = \mu_P$ to $\mu_P = 0$ as the DO_2 concentration falls below the critical value of $DO_{2_{crit_P}}$. This type of relationship was also shown by Hegewald et al. (1981) to successfully model the observed decrease in penicillin production as a result of the DO_2 falling below its critical value.

To account for the effect of the DO_2 falling below 10% air saturation as discussed in Vardar and Lilly (1982). This simulation assumes that for DO_2 concentrations below this value, all cell metabolism ceased and was modelled by relating the DO_2 to specific growth rate of biomass (μ_X), defined here as:

$$\mu_X \approx 0.5\mu_X(1 - \tanh(A_{inhib}(DO_{2_{crit_X}} - DO_2))) \quad (19)$$

where $DO_{2_{crit_X}}$ represents the critical value of DO_2 concentration for biomass. Eq. (19) assumes that provided the DO_2 is above $DO_{2_{crit_X}}$, $\mu_X = \mu_X$, however if DO_2 is less than $DO_{2_{crit_X}}$, μ_X will effectively go to zero with A_{inhib} defined as in Eq. (18).

2.2. Dissolved carbon dioxide

Dissolved carbon dioxide ($CO_{2,L}$) is an important and often overlooked variable in fermentation modelling with accumulation of $CO_{2,L}$ in the broth reported to be detrimental to cell growth and productivity (Frick and Junker, 1999). However lack of accurate and robust analysers has limited its widespread on-line measurement. The dissolved carbon dioxide in fermentations was shown by Royce (1992) to be effected by $k_L a$ as well as the environmental conditions of pH and vessel pressure. The model proposed here assumes the pH effect is negligible as the pH is generally held constant and is modelled as:

$$\frac{dCO_{2,L}}{dt} = \delta_{c/o} k_L a(CO^*_{2,L} - CO_{2,L}) - \frac{CO_{2,L} dV}{V dt} \quad (20)$$

Where $\delta_{c/o}$ is the ratio of the carbon dioxide to oxygen mass transfer coefficient. $C^*_{L_{CO2}}$ is the maximum dissolved carbon dioxide concentration assumed proportional to the off-gas measurement of CO_2 taken as (Royce, 1992):

$$C^*_{L_{CO2}} = \frac{P_{lm} CO_{2_{out}}}{H_{CO_2}} \quad (21)$$

Where $CO_{2_{out}}$ is the percentage concentration of CO_2 in the off-gas, P_{lm} is the log-mean pressure and H_{CO_2} is Henry's law constant for carbon dioxide.

Although the $CO_{2,L}$ was not measured in the case study, the operators used the $CO_{2_{out}}$ in the off-gas analysis to approximate it. This approximation allowed the operators to determine periods where the $CO_{2,L}$ was too high and to take corrective action to avoid the detrimental effect on the biomass and its impact on product formation. To model this relationship, the simulation assumed that provided the $CO_{2,L}$ concentration was below a critical value ($CO_{2,L_{crit_X}}$), the specific growth rate (μ_X) was unaffected. However for $CO_{2,L}$ concentrations above this value, μ_X goes to zero. This was modelled using a hyperbolic tangent function ranging from 0 to 1, defined as:

$$\mu_X \approx 0.5\mu_X(1 + \tanh(A_{inhib}(CO_{2,L_{crit_X}} - CO_{2,L}))) \quad (22)$$

Where $CO_{2,L_{crit_X}}$ represents the critical value of $CO_{2,L}$ and A_{inhib} is defined as in Eq. (18).

2.3. Nitrogen

The second most abundant nutrient in the fermentation media is generally the nitrogen source as it is critical to growth and required for metabolic production of product (Vogel and Todaro, 1997). The primary source of nitrogen for each batch is generally contained in the starting media and consumed throughout the batch. This consumption is modelled using a material balance which considered the nitrogen consumed during biomass growth and maintenance and that utilised for penicillin production, defined as:

$$\frac{dN}{dt} = \frac{F_{oil}c_{N_{oil}} + F_{PAA}c_{N_{PAA}} + N_{shots}c_{N_{shots}}}{V} - \mu_X X Y_{N/X} - \mu_P X Y_{N/P} - m_N X - \frac{N}{V}\frac{dV}{dt} \quad (23)$$

The simulation considers the nitrogen composition of the input feeds, F_{oil} and F_{PAA} in addition to the ammonia sulphate salts (N_{shots}) which are added to rapidly increase the nitrogen concentration. The nitrogen concentration in these inputs (i) is represented by c_{N_i}. The yield coefficients of nitrogen to biomass and penicillin were represented as $Y_{N/X}$ and $Y_{N/P}$, respectively.

The importance of nitrogen as a key macro-molecule for industrial penicillin production was demonstrated in McIntyre et al. (1999), who observed a decrease in biomass growth during periods of nitrogen limitation. Similar finding were observed in the case study, where the biomass growth rate was shown to decrease for concentrations of nitrogen below 200 mg L^{-1}. To model this relationship, the simulation assumed that provided the nitrogen concentration was above a critical value (N_{crit_X}), the specific growth

rate (μ_X) was unaffected. However for nitrogen concentrations below this value, μ_X goes to zero. This was modelled using a hyperbolic tangent function ranging from 0 to 1, defined as:

$$\mu_X \approx 0.5\mu_X(1 - \tanh(A_{inhib}(N_{crit_X} - N))) \quad (24)$$

where, N_{crit_X} was the critical concentration of nitrogen for biomass growth and A_{inhib} is defined as in Eq. (18).

2.4. Precursor addition

Some fermentations require the addition of a precursor to ensure metabolic production of a desired product. This is particularly important for the industrial case study presented here, where phenylacetic acid (*PPA*) is added to supply the desired side chain for penicillin synthesis. Hillenga et al. (1995) have investigated this uptake rate and found *PAA* is absorbed across the cell membrane through passive diffusion and is effected by environmental conditions including pH. However Fernandez-canon et al. (1989) reported that the uptake rate of *PAA* was via a specific transport system and is strictly related to the carbon source. Based on the limited data available in this study the developed simulation ignores the environmental conditions and proposes a simplified *PAA* uptake rate based on the biomass growth, penicillin production and penicillin maintenance, modelled here as:

$$\frac{dPAA}{dt} = \frac{F_{PAA}c_{PAA}}{V} - Y_{PAA/P}\mu_P P - Y_{PAA/X}\mu_X X - m_{PAA}P - \frac{PAA}{V}\frac{dV}{dt} \quad (25)$$

where F_{PAA} is the flow rate of the *PAA* and c_{PAA} is the feed solution concentration. $Y_{PAA/P}$ and $Y_{PAA/X}$ are the yield coefficients of *PAA* for penicillin and biomass, respectively and m_{PAA} is a maintenance term related to the concentration of penicillin.

Optimum control of the F_{PAA} is a major challenge in penicillin fermentations as it is known that high levels of *PAA* in the culture are toxic to the biomass by inhibiting growth and penicillin production (Hillenga et al., 1995). Furthermore, *PAA* is one of the most expensive feedstocks accounting for 11% of all raw material costs (Herschbach et al., 1984), so its addition must be carefully monitored. In the industrial case study the *PAA* concentration was shown to be controlled between an optimum range of between 200 and 2000 mg L^{-1} for all ten batches, through the manipulation of F_{PAA}. Similar optimum ranges were reported in Herschbach et al. (1984). Maintaining the *PAA* within these ranges was assumed to alleviate the inhibition effects of high and low concentrations of *PAA* highlighted by Hillenga et al. (1995). To model this relationship, the simulation included two inhibition terms: the first assumes a decrease in the biomass growth rate for *PAA* concentrations above PAA_{crit_X} (2000 mg L^{-1}) and the second assumes a decrease in the growth rate of penicillin for *PAA* concentrations below PAA_{crit_P} (200 mg L^{-1}). These inhibition terms were modelled here using a hyperbolic tangent function ranging from 0 to 1, defined here as:

$$\mu_X \approx 0.5\mu_X(1 + \tanh(A_{inhib}(PAA_{crit_X} - PAA))) \quad (26)$$

$$\mu_P \approx 0.5\mu_P(1 + \tanh(A_{inhib}(PAA - PAA_{crit_P}))) \quad (27)$$

This relationship assumes that for $PAA > PAA_{crit_X}$, μ_X is effectively zero and for *PAA* concentrations below this value, μ_X was unaffected. Similarly for $PAA < PAA_{crit_P}$, μ_P is effectively zero and for *PAA* concentrations above this value, μ_P was unaffected. A_{inhib} for both equations is defined as in Eq. (18).

2.5. Viscosity

Viscosity is a function of the rheological properties of the fermentation broth. For filamentous fungi, this is dependant on its morphology, characterised as either pellet or filamentous form (Olsvik and Kristiansen, 1994). The pellet form is a result of the branching hyphae intertwining and forming stable aggregates. This form is preferred as it is less viscous, however, nutrient limitation in the pellets can be problematic. The second form is filamentous which results from the long branching hyphae extending to create a complex three dimensional structure. The predominant morphology during each fermentation is dependant on several factors including strain type, spore innoculum concentration and quality, and agitation (Posch et al., 2013). To model this complex process in this work, it was assumed that the concentration of the branching (A_0) region, was associated with the filamentous form and was the only factor related to viscosity. To relate the growth of the A_0 region to the viscosity, it was assumed that the growth of this form could be described using a "cube root" growth relationship, as this growth pattern has been used to describe the growth of pellets in fungi as discussed in Metz and Kossen (1977). A growth lag was added to this relationship to better account for the observed lag in the viscosity recorded for this process. The lag growth model added here was shown to accurately model microbial cell growth in batch cultures by Lin et al. (2000). Additionally the viscosity recorded in the batch records was shown to decrease with the addition of water for injection (F_w). As a result, this effect was included in the model. Although this has not been reported elsewhere, the addition of large volumes of water may aid in the breakup of the viscous filamentous form into smaller aggregates or pellets hence decreasing viscosity. The relationship developed here for the viscosity can be considered as an empirical relationship and does not aim to account for any of the underlying phenomena contributing to broth viscosity, this relationship is defined as:

$$\frac{d\mu_{vis}}{dt} \approx A_0^{\frac{1}{3}}\left(\frac{1}{1 + e^{-k_{in}(t-t_{in})}}\frac{1}{1 + e^{k_{de}(t-t_{de})}}\right) - k_{water}F_w \quad (28)$$

where μ_{vis} is the apparent viscosity and k_{water} is a constant relating to the degree of breakup of the filamentous form as a result of the water addition. The constants k_{in}, t_{in} k_{de} and t_{de} relate to the lag growth model as defined in Lin et al. (2000) with t as the batch time. These values are available in Table 2.

2.6. Temperature and pH

Temperature and pH are both critical process parameters recorded on industrial-scale bioreactors. The modelling of these variables and their control are discussed in Appendix A, Supplementary data.

2.7. Product hydrolysis

Accurate temperature and pH control is not only necessary for continued cell growth and product formation it can also influence the product hydrolysis rate (k). The hydrolysis rate has been previously modelled as a constant (Bajpai and Reul, 1980; Birol et al., 2002; Tiller et al., 1994; Paul and Thomas, 1996). However it has been shown that the degradation of penicillin is a function of both temperature and pH (Kheirolomoom et al., 1999; Lu et al., 2008) and can be modelled using a second order polynomial as defined by Kheirolomoom et al. (1999):

$$\log(k) = B_1 + B_2 pH + B_3 T_b + B_4 pH^2 + B_5 T_b^2 \quad (29)$$

where the constants $B_{1,2,3,4,5}$ (available in Table 2) were modified in the simulation to give a hydrolysis rate of ≈ 0.003 h^{-1} at a pH of 6.5 and a temperature of 298 K to equal the value originally proposed in Paul and Thomas (1996).

2.8. Off-gas analysis

Off-gas analysis involves monitoring the exhaust gas leaving the head space of the fermenter. It is a non-invasive process that does not compromise the sterility of the culture, offering a clear advantage over in-situ probes which contact the broth. The technique involves monitoring the concentrations of the CO_2 and O_2, in the inlet and outlet gas streams. The off-gas concentration of oxygen ($O_{2_{out}}$), was measured in terms of % here and was adapted from Scragg (1991) as:

$$\frac{dO_{2_{out}}}{dt} = (Q_{g_{in}} O_{2,in} - Q_{g_{out}} O_{2,out} - k_L a(DO_2^* - DO_2)V_L)/(29V_g/22.4) \quad (30)$$

where $Q_{g_{in}}$ and $Q_{g_{out}}$ is taken as the mass flow rate of air in and out, respectively. $Q_{g_{out}}$ was determined by preforming a mass balance on the inert gas nitrogen as in Eq. (32). $O_{2_{in}}$ and $O_{2_{out}}$ are the oxygen concentrations in the inlet and gas outlet, respectively. V_g is the volume of the gas in the vessel taken as εV_L which is converted into a mass here to work out $O_{2_{out}}$ in terms of %. Similarly, the off-gas calculation of CO_2 was calculated as:

$$\frac{dCO_{2_{out}}}{dt} = (Q_{g_{in}} CO_{2,in} - Q_{g_{out}} CO_{2,out} + CER_X)/(29V_g/22.4) \quad (31)$$

where the CER_X is the carbon evolution rate taken here as directly related to the biomass: $CER_X = VX/Y_{CO_2-X}$ with Y_{CO_2-X} as the yield coefficient of CO_2 (Scragg, 1991). Measuring the CO_2 and O_2 concentrations in the off-gas analysis allows for the calculation of the oxygen uptake rate (*OUR*) and the carbon evolution rate (*CER*) which are valuable tools in the real-time monitoring of fermentations, calculated from Scragg (1991) as:

$$OUR = \frac{32}{22.4} F_{g_{in}} \left(O_{2_{in}} - O_{2_{out}} \frac{N_{2_{in}}}{1 - O_{2_{out}} - CO_{2_{out}}} \right)$$
$$CER = \frac{44}{22.4} F_{g_{in}} \left(CO_{2_{out}} \frac{N_{2_{in}}}{1 - O_{2_{out}} - CO_{2_{out}}} - CO_{2_{in}} \right) \quad (32)$$

2.9. Summary of growth inhibition terms

The finalised specific growth of biomass is defined as:

$$\mu_X = \mu_X(DO_{2Xinhib})(dCO_{2inhib})(N_{inhib})(PAA_{Xinhib})(T_{inhib})(pH_{inhib}) \quad (33)$$

where $DO_{2Xinhib}$ is the inhibition effect of dissolved oxygen on the biomass specific growth rate defined in Eq. (19). Similarly, dCO_{2inhib}, is defined by Eq. (22), N_{inhib} by Eq. (24), PAA_{Xinhib} by Eq. (26), T_{inhib} by Eq. (A-3) and pH_{inhib} by (A-10).

Likewise the finalised specific production rate of penicillin is defined as:

$$\mu_P = \mu_P(DO_{2Pinhib})(PAA_{Pinhib}) \quad (34)$$

where $DO_{2Pinhib}$ is the inhibition effect of dissolved oxygen on the penicillin production rate defined in Eq. (18) with PAA_{Pinhib} defined by Eq. (27).

3. Case study: industrial-scale penicillin production

The simulation was validated using a case study consisting of the batch records from ten penicillin fermentations carried out in an industrial-scale bioreactor.

3.1. Materials and methods

The industrial penicillin fermentation was carried out in a 100,000 L bioreactor using an industrial strain of *P. chrysogenum*. The initial inoculum charge for this production facility was generated using two seed stages, a primary (1000 L) and secondary (10,000 L) seed vessel. Specific details regarding strain selection, media composition and analytical methods have been omitted for reasons of confidentiality.

3.2. Process description and operation

The configuration of the bioreactor was consistent with the traditional 100,000 L bioreactor available in Shuler and Kargi (2002), shown in Fig. 2. The bioreactor had a tank radius (r) of 2.1 m with three rushton impellers each with an internal radius (r_{imp}) of 0.85 m and was operated at a fixed agitation of 100 rpm. The vessel was equipped with pH, temperature, dissolved oxygen, foaming and pressure sensors. Off-line measurements of penicillin, nitrogen and viscosity were sampled and collected every 24 h whilst the off-line phenylacetic acid measurements were taken every 12 h. Further to this, concentrations of oxygen and carbon dioxide were monitored through off-gas analysis. Feed rates of soybean oil and substrate were controlled through sequential batch control using a predetermined optimum profile, manually adjusted throughout the batch by the operators in response to process behaviour. Similarly, both the aeration rate and vessel back pressure were manipulated using sequential batch control to maintain the desired dissolved oxygen concentration level as well responding to process issues including foaming and high $CO_{2_{out}}$ levels. Soybean oil was utilised as a secondary carbon source as well as acting as an anti-foaming agent. Phenylacetic acid flow was manually adjusted based on off-line measurements of its concentration. Nitrogen was present in the starting medium of each batch and monitored throughout using off-line measurements. Low levels of nitrogen were rectified through the addition of ammonia sulphate shots. Coolant through internal cooling coils, and addition of acid/base solutions were used to control the temperature at 298 K and pH at 6.5, respectively, using PID controllers. Vessel weight was recorded on-line using a load cell which was used to schedule discharges to ensure that the capacity of the bioreactor was not exceeded, these discharges also allow for longer batches to be achieved.

3.3. Fermentation data

The batch records summarised in Table 3 were used for parameter estimation and to validate the simulation. These records highlight the typical batch to batch variation found on this facility including some process related problems that were commonly encountered. The case study therefore provides ideal data to validate the simulation. The batch lengths were based on the current batch progression and also dependant on the availability of the downstream processing unit operations. The maximum specific growth rates of biomass ($\mu_{X_{max}}$) were calculated from the estimated biomass (X_{est}) using the carbon evolution rate (*CER*), defined as:

$$\frac{dX_{est}}{dt} = \frac{CER - m_{CO_2} X_{est}}{Y_{CO_2/X}} \quad (35)$$

where m_{CO_2} is the maintenance production term for CO_2 and $Y_{CO_2/X}$ is the CO_2 yield coefficient. Both the carbon evolution rate (*CER*) and the oxygen uptake rate (*OUR*) can be used here for the on-line estimation of the biomass. However use of the *CER* measurement is preferred among fermentation technologists (Royce, 1992). Additionally, Table 3 highlights the variation associated with the maximum specific growth rates of penicillin ($\mu_{P_{max}}$) which were calculated from the first three off-line penicillin measurements from each batch. The main process inputs and outputs, highlighted in Fig. 2, were recorded hourly during each batch. The cooling water and acid/base flow rates were not made available for this study.

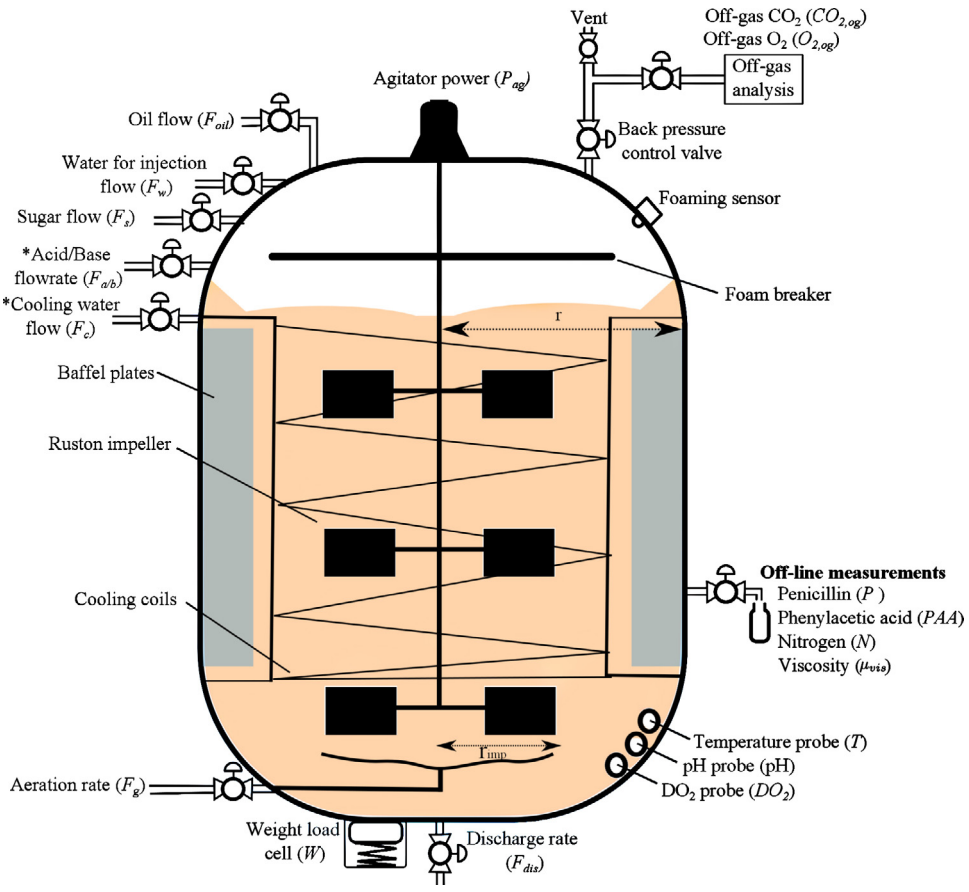

Fig. 2. Schematic of the 100,000 L bioreactor used, with all the process inputs and outputs. The variables marked with the asterisk represent the variables not recorded by the batch records.

3.4. Parameter estimation

Parameters for the simulation are expected to be strongly strain dependant and process specific. However as some parameters could not be estimated from the batch records it was considered sufficient to estimate these parameters from relevant literature sources. Some parameters including the critical limits of oxygen, nitrogen and phenylacetic acid were based on the process information gathered from the operators of this facility. The parameters relating to the penicillin model are summarised in Table 1A; process parameters relating to the environmental conditions are summarised in Table 2 with the remaining available in Table 2A. The PID controller limits and gains are available in Table 3A. No attempt was made to optimise the given parameter set as these parameters were shown to give a reasonable prediction of the main process outputs in comparison to those recorded for all ten batches of the case study.

3.5. Sensitivity analysis

Sensitivity analysis was performed on all the simulation parameters to study the effect of uncertainty of these inputs on the simulation. The sensitivity measure, δ^{msqr}, was used to rank the significance of each parameter, θ, as outlined in Sin et al. (2009). The 10 highest ranking parameters that effected the six primary outputs of the simulation are summarised in Table 4.

Certain parameters were shown to be highly influential on a large number of outputs. Among these parameters were the inlet concentrations of the substrate, c_s, and oil, c_{oil}, which in this work were assumed constant as no measurements of input

Table 3
Summary of the 10 industrial-scale penicillin fermentations studied in this present work. The average and standard deviations are shown for the batch length (t), the maximum specific growth rate of biomass ($\mu_{X_{max}}$) and the maximum specific growth rate of penicillin ($\mu_{P_{max}}$).

Run	Vessel	t (h)	$\mu_{X_{max}}$ (h^{-1})	$\mu_{P_{max}}$ (h^{-1})	Observations
Batch 1	V-1	211	0.4136	0.0504	Typical fermentation
Batch 2	V-3	286	0.4360	0.0479	Foaming
Batch 3	V-1	317	0.4196	0.0444	Typical fermentation
Batch 4	V-3	133	0.4282	0.0414	Substrate pump failure
Batch 5	V-3	257	0.3234	0.0409	High CO_2
Batch 6	V-3	241	0.4168	0.0480	Sparger blown &foaming
Batch 7	V-5	217	0.4529	0.0489	NH_3 limitation
Batch 8	V-4	218	0.4201	0.0439	Typical fermentation
Batch 9	V-1	272	0.4106	0.0374	Poor Temp control
Batch 10	V-2	209	0.2773	0.0459	NH_3 limitation
Average		236.1 ± 48	0.400 ± 0.0521	0.0449 ± 0.00389	

Table 4
The 10 highest ranking parameters of six model out-puts based on the sensitivity measure δ^{msqr}.

Rank	Biomass		Penicillin		Substrate		DO_2		Temp		CO_2 off-gas	
	θ	δ^{msqr}	θ	δ^{msqr}	θ	δ^{msqr}	θ	δ^{msqr}	θ	δ^{msqr}	θ	δ^{msqr}
1	c_s	0.41	$\mu_{P_{\max}}$	0.83	$\mu_{X_{\max}}$	25.21	H_{O_2}	0.15	T_{cin}	0.34	$Y_{CO_2/X}$	0.66
2	K_d	0.30	c_s	0.41	$Y_{s/X}$	14.42	$O_{2,in}$	0.15	β_1	0.24	c_s	0.35
3	$Y_{s/X}$	0.29	$Y_{s/X}$	0.31	c_{oil}	0.46	r	0.14	$Y_{Q/X}$	0.23	K_d	0.32
4	β_1	0.27	$\frac{\mu_e}{\mu_b}$	0.31	$\frac{\mu_e}{\mu_b}$	0.07	r_{imp}	0.07	$\mu_{X_{\max}}$	0.22	$Y_{s/X}$	0.08
5	$\mu_{P_{\max}}$	0.21	K_b	0.22	c_s	0.07	d	0.51	r_{imp}	0.16	β_1	0.06
6	m_s	0.10	m_s	0.18	K_b	0.009	a	0.05	K_d	0.084	$\mu_{P_{\max}}$	0.55
7	c_{oil}	0.09	$s_{P}^{\max}$	0.15	m_s	0.009	α_{k_La}	0.02	$Y_{s/X}$	0.06	m_s	0.04
8	$Y_{s/P}$	0.05	c_{oil}	0.14	K_e	0.006	m_{O_2X}	0.02	β_T	0.04	c_{oil}	0.04
9	K_e	0.02	$\mu_{X_{\max}}$	0.13	K_d	0.004	b	0.02	$\frac{\mu_e}{\mu_b}$	0.01	$Y_{s/P}$	0.03
10	$\frac{\mu_e}{\mu_b}$	≈ 0	K_v	0.001	β_1	≈ 0	K_d	0.01	c_{oil}	0.001	K_e	0.004

concentrations were available. $\mu_{X_{\max}}$ and $\mu_{P_{\max}}$ were calculated for each batch and these parameters were shown to have a significant influence on both the substrate and penicillin concentrations. Interestingly, $\mu_{X_{\max}}$ was not shown to have a significant effect on the biomass which may explain why the biomass profiles of each batch were relatively similar despite the large variations in the value of these parameters as highlighted in Table 3. Table 4 also highlights the importance of the manipulated variables, such as the inlet coolant temperature, T_{cin}, and the sparged oxygen inlet gas concentration, $O_{2_{in}}$, and their large influence on the process outputs of temperature and dissolved oxygen, respectively. Furthermore the vessel dimensions were shown to influence certain model outputs; with the impeller radius (r_{imp}) and vessel radius (r) influencing the dissolved oxygen concentration (DO_2).

3.6. Industrial penicillin simulation

The simulation was validated using the batch records from the industrial case study. This was carried out by initialising the simulation with the starting conditions defined in each of the batch records for the dissolved oxygen, temperature, pH, phenylacetic acid, nitrogen, penicillin, vessel weight, viscosity and off-gas concentrations of oxygen and carbon dioxide. The initial substrate concentration was taken as 1 g L^{-1} and the initial dissolved carbon dioxide was taken as 0 g L^{-1}. The starting biomass concentration was assumed to be constant for each batch and was taken as 0.5 g L^{-1}. The maximum specific growth rates of biomass ($\mu_{X_{\max}}$) and penicillin ($\mu_{P_{\max}}$) provided in Table 3 were used as model inputs for each batch. The batch length (t) as determined by the batch records was used to define the simulation run time. The manipulated variables were the sugar flow (F_s), soybean oil flow (F_{oil}), water for injection (F_w), aeration rate (F_g), vessel back pressure (P_1) and discharge rate (F_{dis}). These variables were interpolated using a sample rate of 0.2 h and used as the simulation inputs. The simulation assumed the vessel was operated using a fixed agitation of 100 rpm which was consistent with the normal operation of the industrial process. As the acid/base and coolant flow rates were not made available for this study, these were taken as the outputs of the PID controllers operating in closed loop to maintain the process at its optimum pH of 6.5 and temperature of 298 K. The outputs of the simulation were the biomass (X), penicillin (P), substrate (s), dissolved oxygen (DO_2), temperature (T), pH, weight (W), viscosity (μ_{app}), phenylacetic acid (PAA), nitrogen (NH_3), dissolved carbon dioxide ($CO_{2,L}$) and the off-gas concentrations of oxygen ($O_{2_{out}}$) and carbon dioxide ($CO_{2,out}$). The off-gas concentrations were used to calculate the carbon dioxide evolution rate (CER) and the oxygen uptake rate (OUR) using Eq. (32). Where available all predictions from the simulator were compared with those recorded in the batch records.

4. Results and discussion

Fig. 3 highlights the predictive capability of the simulation through the comparison of six selected outputs from Batch 3 (the longest available batch) against the batch records using the nominal parameter set. In contrast to previous simulations validated using fermentation data carried out in relativity small volumes (V = 2 L in (Paul and Thomas, 1996) and (Paul et al., 1998) and V = 1000 L in Menezes and Alves (1994)). The simulated predictions shown here, are valid for fermentations carried out in industrial-scale bioreactors (volume = 100,000 L). Additionally, the simulation was shown to give accurate predictions for batches up to 320 h in comparison to previous simulations validated using data with shorter batch lengths (t = 160 in (Paul and Thomas, 1996), t = 90 in Megee et al. (1970) and t = 200 in Tiller et al. (1994)). Similar predictions were recorded for the remaining nine batches.

The penicillin model proposed in this paper provides accurate predictions of the biomass (X) and penicillin (P), when compared with measurements recorded from the industrial process. The determination of K_{diff} as defined in Eq. (10), results in an increase in the biomass growth rate at the start of the batch as well as the observed decrease after hour 150. This behaviour was found to agree with the biomass profile (estimated using Eq. (35)) shown in Fig. 3A).

The majority of the previously published penicillin simulations Paul and Thomas (1996), Tiller et al. (1994), Megee et al. (1970), Birol et al. (2002) primarily focused on modelling the biomass, penicillin and substrate. The simulation proposed here also includes predictions of the nitrogen (N) and phenylacetic acid (PAA), shown in Fig. 3(C) and (D), respectively. The prediction of these variables is shown to adequately fit the off-line measurements recorded in the batch records. However, the consumption rates of these key nutrients, defined in Eqs. (23) and (25) were found to be highly sensitive to the composition of nitrogen ($c_{N_{PAA}}$) and phenylacetic acid ($c_{N_{PAA}}$) in the phenylacetic acid feed (F_{PAA}). To obtain accurate predictions of these nutrients for all ten batches, deviations in the inlet concentrations of the phenylacetate acid feed was assumed, as defined in Table 2. Deviations in the raw material composition of these materials is expected for industrial fermentations (Posch et al., 2012). However there were no measurements of these raw materials available and hence these assumed deviations could not be validated. The inclusion of these key nutrients allows for controllers to be developed for this simulation that consider the realistic challenges that are faced when nutrients are controlled using off-line measurements. This has been highlighted as a key challenge in the biotechnology sector (Alford, 2006).

The simulation takes into account the growing interest in the application of soft sensors in bioprocess control (Luttmann et al., 2012), through the inclusion of off-gas concentrations of oxygen

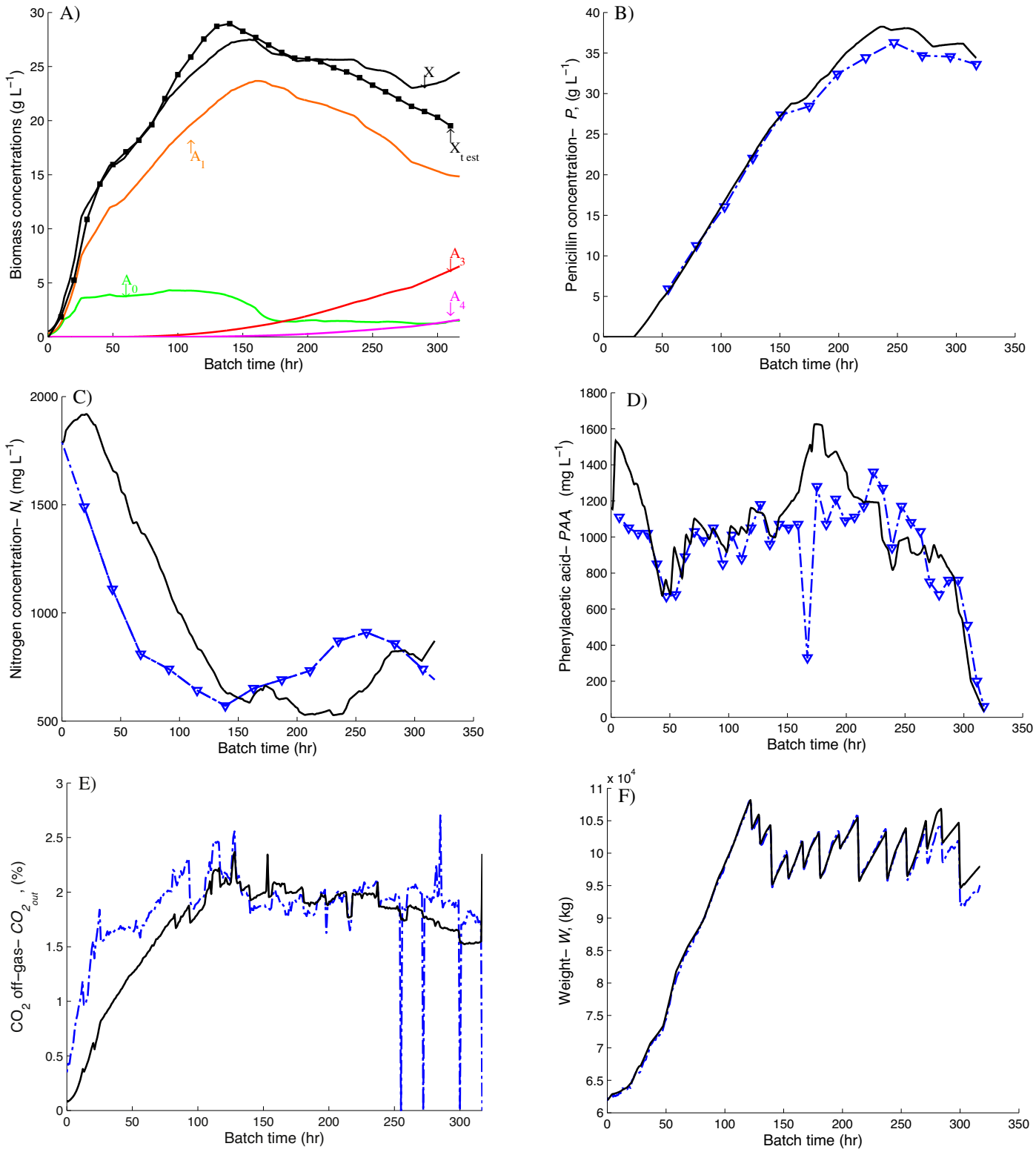

Fig. 3. Simulation predictions of the primary process parameters for Batch 3. (A) The four biomass regions: A_0 – growing region, A_1 – non-growing region A_3 – degenerated region and A_4 – autolysed regions with the total biomass taken as $X = A_0 + A_1 + A_3 + A_4$ represented by – and the biomass estimated from the *CER* (X_{est}) is represented by —■—. Graphs (B)-> (F) Comparison of the model predictions (represented by –) against those recorded in the batch records (represented by —•—) for penicillin (P), nitrogen (N), phenylacetic acid (*PAA*), CO_2 off gas ($CO_{2_{out}}$) and weight (*W*). In graphs B), C) and D) the off-line measurements recorded from the batch records of penicillin, nitrogen and phenylacetic acid are represented by –▼–.

($O_{2_{out}}$) and carbon dioxide ($CO_{2_{out}}$). The simulation improves on the $CO_{2_{out}}$ developed in Birol et al. (2002) by considering the effect of the gas flow rates into and out of the vessel as discussed in section 2.8. These predictions are in close agreement with those recorded in the batch records, as shown by the accuracy of the $CO_{2_{out}}$ measurement shown in Fig. 3E).

Unlike previous fermentation simulations, which were mainly operated as fed-batch processes, the simulation proposed here was

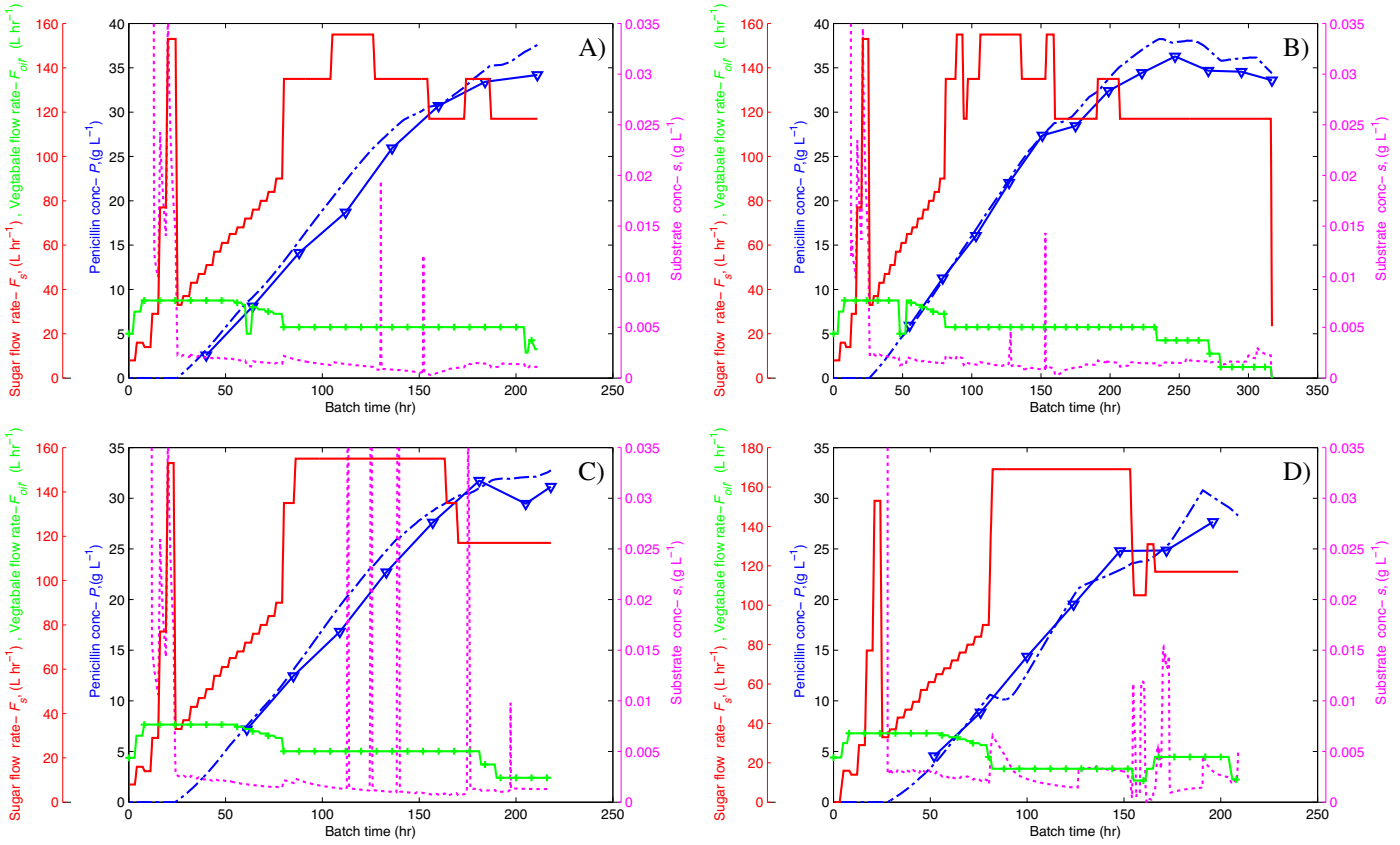

Fig. 4. Prediction capability of the simulation for four bathes. (A) Batch 1, (B) Batch 3, (C) Batch 8 and (D) Batch 10. The recorded industrial data for substrate feed (F_s) is represented as ——, the soybean oil feed rate (F_{oil}) as +, and the off-line penicillin measurements as —▽—. The simulated results of the penicillin (P) is represented as — · —, and substrate concentration (s) as . . . .

shown to operate using a repeated fed-batch operation as highlighted in Fig. 3F). This type of operation is a common operating strategy for industrial penicillin fermentations (Pirt, 1974). This strategy involves scheduled discharges from the fermenter, based on the vessel weight, to ensure the capacity of the bioreactor was not exceeded and to allow for extended penicillin production times. The weight profile shown in Fig. 3F) was calculated using Eq. (8) and the densities of the process inputs and outputs as defined in Table 2A.

Fig. 4 compares the model predictions of Batches 1, 3, 8 and 10 against those recorded in the batch records using the nominal parameter set, with the exception of the specific growth rates of biomass and penicillin which were taken from Table 3. The control strategy implemented on this facility was predominately sequential batch control. This control strategy standardises the input flow rates based on a predefined optimum profile. The sharp increase observed in F_s at hour 20 for all batches ensures the substrate concentration is in excess and the biomass remains in its "rapid-growth" phase during the start of each batch. The subsequent decrease in F_s switches the batch to its productive phase, where the substrate concentration is maintained at a minimum to maximise penicillin production, with similar operation reported in Montague et al. (1986). The accuracy of the simulation to predict the penicillin profile is enhanced through the use of the $\mu_{P_{\max}}$ as a model input. This parameter was shown in the sensitivity analysis to have the biggest influence on the penicillin production.

A limitation of the proposed simulation is its ability to accurately predict the dissolved oxygen (DO_2) and viscosity (μ_{app}). The primary process inputs which influence both of these variables are highlighted in Fig. 5. The prediction of the DO_2 compared with the recorded measurements is shown shown in Fig. 5C). This figure shows the prediction is reasonably accurate, however deviations are evident, particularly during the beginning of the batch. This deviation can be attributed to the large discrepancy between the simulated viscosity and that recorded off-line on the industrial process. An improved prediction of the DO_2 is obtained using the recorded viscosity as a process input to the simulation. However, as the viscosity is related to a large number of factors (discussed in Section 2.5) which were not recorded on this facility, the proposed model for viscosity given in Eq. (28) is sufficient for the proposes of the simulation. This viscosity term can be used to simulate the typical challenges associated with control of dissolved oxygen during highly viscous fermentations.

In addition to the results discussed here, the simulation also contained PID controllers to regulate the temperature and pH. The resulting predictions of the temperature and pH were found to be in good agreement with the profiles recorded by the batch records, shown in the appendix in Fig. 3A. It must be noted that due to the large working volume of industrial scale bioreactors (<100 m^3) and the highly viscous nature of filamentous fungi broths, mixing times within these fermentations were reported to range from one to several minutes (De Jonge et al., 2011). This may result in an inhomogeneous distribution of pH, temperature and DO_2. Therefore these process measurements, recorded using a single sensor may not provide an accurate representation of the whole bioreactor, which may have introduced errors into the model, which assumes a perfectly mixed vessel.

The dissolved carbon dioxide (CO_{2_L}) was predicted by the simulation to account for the inhibiting effect of high CO_{2_L} on the biomass as discussed in Section 2.2. An example of this inhibition is shown in Batch 5.

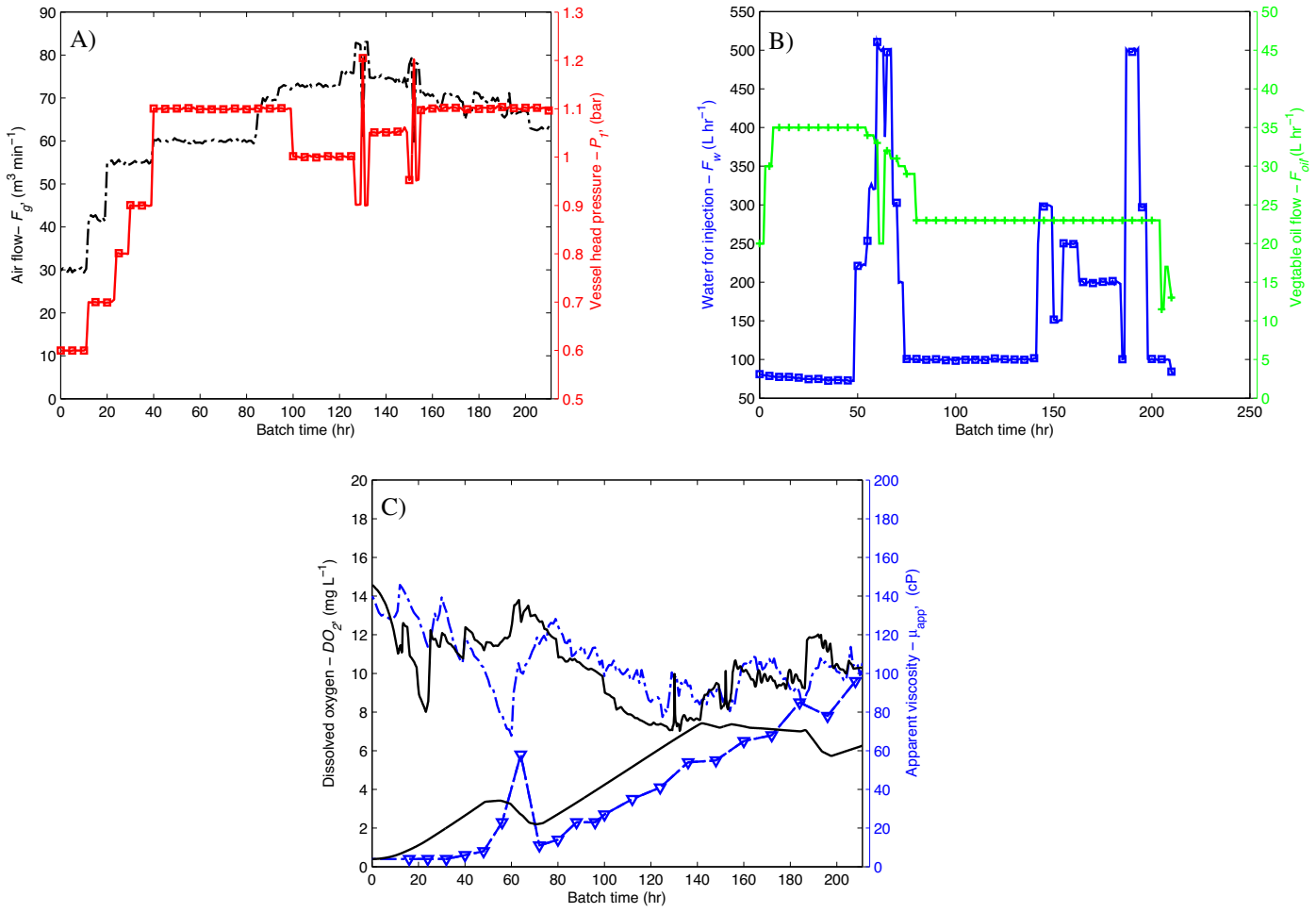

Fig. 5. Input variables (Batch 1) related to the dissolved oxygen (DO_2) and viscosity (μ_{app}), with aeration rate (F_g) represented as -·, vessel back pressure (P_1), —■—, water for injection (F_w), —■— and soybean oil feed rate (F_{oil}), +. For the dissolved oxygen and viscosity, the model predictions are represented by –, and the industrial data as —. with the off-line measurements of viscosity represented as —▼—.

It is often argued that structured models are only applicable in highly instrumented laboratory-scale bioreactors where stable, highly sensitive and accurate measurements can be taken (Menezes and Alves, 1994). This simulation clearly demonstrates the ability of structured models to describe complex industrial processes using routine and commonly recorded measurements.

5. Industrial scale penicillin simulation – IndPenSim

The simulation, referred to as *IndPenSim*, was coded in Matlab R2013b and is available to download at www.industrialpenicillinsimulation.com where the batch records are also available. *IndPenSim* can also be used as a standalone application and aims to replicate the operation of an industrial-scale penicillin fermentation by including the following capabilities:

- Batch to batch variation of $\mu_{X_{max}}$ and $\mu_{P_{max}}$ as well as in-batch fluctuations.
- Option to add disturbances on inlet concentrations of the substrate (c_s), oil (c_{oil}), acid/base molar concentration ($c_{a/b}$) and phenylacetic acid concentration (c_{PAA}).
- Ability to adjust the current sequential batch control strategy for F_s, F_{oil}, F_g, RPM, F_{dis} and F_{PAA}.
- Option to include inhibition effects on the growth rates during DO_2, N and PAA limitation as well as during excessive PAA and CO_{2_L} concentrations and during sub-optimal T and pH ranges.
- Includes a pre-defined delay (3 h) in the off-line measurements of P, N, PAA and μ_{app}.
- Option to include inability of growth rates of biomass and penicillin to return to normal after continuous periods of suboptimal pH and temperature conditions.
- Option to include process faults including agitator trip, aeration faults and sensor errors.

The simulation aims to provide a platform for use in the development of robust control and monitoring strategies for industrial fermentation processes.

6. Conclusion

The successful implementation of a first principles mathematical simulation to a challenging industrial-scale fermentation has been presented. The simulation was shown to capture the complex process dynamics and account for some of the typical faults associated with a modern day biotechnology facility. The simulation incorporated a time varying structured kinetic model that accurately models the biomass and penicillin as well as the main process variables of an industrial-scale fermentation process. The model developed here may serve as a valuable tool in the development

of improved control strategies for industrial fermentations and can also be used for research and educational activities in monitoring, control and optimisation studies.

Acknowledgements

This work was supported by the EPSRC grant (EP/G037620/1) as part of an Engineering Doctorate for SG in Biopharmaceutical Process Development at Newcastle University with financial support and assistance from Perceptive Engineering Ltd.

Appendix A. Supplementary data

Supplementary data associated with this article can be found, in the online version, at http://dx.doi.org/10.1016/j.jbiotec.2014.10.029.

References

Albaek, M.O., Gernaey, K.V., Hansen, M.S., Stocks, S.M., 2012. Evaluation of the energy efficiency of enzyme fermentation by mechanistic modeling. Biotechnol. Bioeng. 109, 950–961.
Alford, J.S., 2006. Bioprocess control: advances and challenges. Comput. Chem. Eng. 30, 1464–1475.
Ashoori, A., Moshiri, B., Khaki-Sedigh, A., Bakhtiari, M.R., 2009. Optimal control of a nonlinear fed-batch fermentation process using model predictive approach. J. Process Control 19, 1162–1173.
Bajpai, R.K., Reul, M., 1980. A mechanistic model for penicillin production. J. Chem. Technol. Biotechnol. 30, 332–344.
Birol, G., Ündey, C., Çinar, A., 2002. A modular simulation package for fed-batch fermentation: penicillin production. Comput. Chem. Eng. 26, 1553–1565.
Chern, J.-M., Chou, S.-R., Shang, C.-S., 2001. Effects of impurities on oxygen transfer rates in diffused aeration systems. Water Res. 35, 3041–3048.
Christensen, L.H., Henriksen, C., Nielsen, J., Villadsen, J., Egel-Mitani, M., 1995. Continuous cultivation of *Penicillium chrysogenum*. Growth on glucose and penicillin production. J. Biotechnol. 42, 95–107.
De Jonge, Lodewijk, P., Buijs, N.A.A., ten Pierick, A., Deshmukh, A., Zhao, Z., Kiel, J.A.K.W., Heijnen, J.J., van Gulik, W.M., 2011. Scale-down of penicillin production in *Penicillium chrysogenum*. Biotechnol. J. 6, 944–958.
Fernandez-canon, J.M., Reglero, A., Martinez-blanco, H., Luengo, J.M., 1989. Uptake of phenylacetic acid by *Penicillium chrysogenum* Wis54-1255: a critical regulatory point in benzylpenicillin biosynthesis. J. Antibiot. 42, 1398–1409.
Finn, R.K., 1954. Agitation–aeration in the laboratory and in the industry. Bact. Rev. 18, 254–274.
Frick, R., Junker, B., 1999. Indirect methods for characterization of carbon dioxide levels in fermentation broth. J. Biosci. Bioeng. 87, 344–351.
Garcia-Ochoa, F., Gomez, E., 2009. Bioreactor scale-up and oxygen transfer rate in microbial processes: an overview. Biotechnol. Adv. 27, 153–176.
Grabowski, H.G., Vernon, J.M., Thomas, L.G., 1978. Estimating the effects of regulation on innovation: an international comparative analysis of the pharmaceutical industry. J. Law Econ. 21, 133–163.
Green, W.D., Perry, H.R., 2008. Perry's Chemical Engineers Handbook. The McGraw Hill.
Hegewald, E., Wolleschensky, B., Guthke, R., Neubert, M., Knorre, W.A., 1981. Instabilities of product formation in a fed-batch culture of *Penicillium chrysogenum*. Biotechnol. Bioeng. 23, 1563–1572.
Herschbach, G.J.M., Van der Beek, C.P., Van Dijck, P.W.M., 1984. The Penicillins: Properties, Biosynthesis, and Fermentation. Marcel Dekker AG.
Hillenga, D.J., Versantvoort, H., Molen, S.V.D., Driessen, A., Konings, W.N., 1995. *Penicillium chrysogenum* takes up the penicillin G precursor phenylacetic acid by passive diffusion. Appl. Environ. Microbiol. 61, 2589–2595.
Junker, B., 2007. Foam and its mitigation in fermentation systems. Biotechnol. Prog. 23, 767–784.
Kawase, Y., Moo-Young, M., 1990. The effect of antifoam agents on mass transfer in bioreactors. Bioprocess Eng. 5, 169–173.
Kheirolomoom, A., Kazemi-Vaysari, A., Ardjmand, M., Baradar-Khoshfetrat, A., 1999. The combined effects of pH and temperature on penicillin G decomposition and its stability modeling. Process Biochem. 35, 205–211.
Lee, J.-M., Yoo, C.K., Lee, I.-B., 2004. Enhanced process monitoring of fed-batch penicillin cultivation using time-varying and multivariate statistical analysis. J. Biotechnol. 110, 119–136.
Lin, J., Lee, S.-M., Lee, H.-J., Koo, Y.-M., 2000. Modeling of typical microbial cell growth in batch culture. Biotechnol. Bioprocess Eng. 5, 382–385.
Lu, X., Xing, H., Su, B., Ren, Q., 2008. Effect of buffer solution and temperature on the stability of Penicillin G. J. Chem. Eng. Data 53, 543–547.
Luttmann, R., Bracewell, D.G., Cornelissen, G., Gernaey, K.V., Glassey, J., Hass, V.C., Kaiser, C., Preusse, C., Striedner, G., Mandenius, C.-F., 2012. Soft sensors in bioprocessing: a status report and recommendations. Biotechnol. J. 7, 1040–1048.
McIntyre, M., Berry, D.R., McNeil, B., 1999. Response of *Penicillium chrysogenum* to oxygen starvation in glucose- and nitrogen-limited chemostat cultures. Enzyme Microb. Technol. 25, 447–454.
Megee, R.D., Kinoshita, S., Fredrickson, a.G., Tsuchiya, H.M., 1970. Differentiation and product formation in molds. Biotechnol. Bioeng. 12, 771–801.
Menezes, J.C., Alves, S.S., 1994. Mathematical modelling of industrial pilot-plant Penicillin-G fed-batch fermentations. J. Chem. Technol. Biotechnol. 61, 123–138.
Metz, B., Kossen, N.W.F., 1977. The growth of molds in the form of pellets – a literature review. Biotechnol. Bioeng. XIX, 781–799.
Montague, G.A., Morris, A.J., Wright, A.R., Aynsley, M., Ward, A., 1986. Modelling and adaptive control of fed-batch penicillin fermentation. Can. J. Chem. Eng. 64, 567–580.
Nestaas, E., Wang, D.I.C., 1983. Computer control of the penicillin fermentation using the filtration probe in conjunction with a structured process model. Biotechnol. Bioeng. 25, 781–796.
Nielsen, J., 1993. A simple morphologically structured model describing the growth of filamentous microorganisms. Biotechnol. Bioeng. 41, 715–727.
Nielsen, J.H.i., Villadsen, J., Lidén, G., 2003. Bioreaction Engineering Principles. Kluwer Academic/Plenum Publishers.
Olsvik, E., Kristiansen, B., 1994. Rheology of filamentous fermentations. Biotechnol. Adv. 12, 1–39.
Patnaik, P.R., 2001. Penicillin fermentation: mechanisms and models for industrial-scale bioreactors. Crit. Rev. Microbiol. 27, 25–39.
Paul, G., Syddall, M., Kent, C., Thomas, C., 1998. A structured model for penicillin production on mixed substrates. Biochem. Eng. J. 2, 11–21.
Paul, G.C., Thomas, C.R., 1996. A structured model for hyphal differentiation and penicillin production using *Penicillium chrysogenum*. Biotechnol. Bioeng. 51, 558–572.
Pirt, S., 1974. The theory of fed batch culture with reference to the penicillin fermentation. J. Appl. Chem. Biotechnol. 24, 415–424.
Posch, A.E., Herwig, C., Spadiut, O., 2013. Science-based bioprocess design for filamentous fungi. Trends Biotechnol. 31, 37–44.
Posch, A.E., Spadiut, O., Herwig, C., 2012. Switching industrial production processes from complex to defined media: method development and case study using the example of *Penicillium chrysogenum*. Microb. Cell Fact. 11, 88–102.
Righelato, R.C., Trinci, a.P., Pirt, S.J., Peat, A., 1968. The influence of maintenance energy and growth rate on the metabolic activity, morphology and conidiation of *Penicillium chrysogenum*. J. Gen. Microbiol. 50, 399–412.
Roels, J.A., Heijnen, J.J., 1980. Power dissipation and heat production in bubble columns: approach based on nonequilibrium thermodynamics. Biotechnol. Bioeng. 22, 2399–2404.
Rolinson, N.G., 1952. Respiration of *Penicillium chrysogenum* in penicilllin fermentations. J. Gen. Microbiol. 6, 336–343.
Routledge, S.J., 2012. Beyond de-foaming: productivity the effects of antifoams on bioprocess productivity. Comput. Struct. Biotechnol. J. 3, 1–7.
Royce, P.N., 1992. Effect of changes in the pH and carbon dioxide evolution rate on the measured respiratory quotient of fermentations. Biotechnol. Bioeng. 40, 1129–1138.
Scragg, A.H., 1991. Bioreactors in Biotechnology: A Practical Approach. Ellis Horwood Limited.
Seborg, D.E., Edgar, T.F., Mellichamp, D.A., 2004. Process Dynamics & Control. John Wiley & Sons.
Shinskey, G.E., 1973. pH and pION Control in Process and Waste Streams. John Wiley & Sons.
Shuler, M.L., Kargi, F., 2002. Bioprocess Engineering: Basic concepts. Prentice Hall PTR.
Sin, G., Gernaey, K.V., Lantz, A.E., 2009. Good modeling practice for PAT applications: propagation of input uncertainty and sensitivity analysis. Biotechnol. Prog. 25, 1043–1053.
Syndall, T.M., (Ph.D. thesis) 1998. Improving the identification of a Penicillin fermentation model. University of Birmingham.
Tiller, V., Meyerhoff, J., Sziele, D., Schügerl, K., Bellgardt, K.H., 1994. Segregated mathematical model for the fed-batch cultivation of a high-producing strain of *Penicillium chrysogenum*. J. Biotechnol. 34, 119–131.
Uhl, V.M., Gray, B.J., 1966. Mixing – Theory and Practice. Academic Press, New York.
Ündey, C., Ertunç, S., Çinar, A., 2003. Online batch/fed-batch process performance monitoring, quality prediction, and variable-contribution analysis for diagnosis. Ind. Eng. Chem. Res. 42, 4645–4658.
Vardar, F., Lilly, M.D., 1982. Effect of cycling dissolved oxygen concentrations on product formation in penicillin fermentations. Eur. J. Appl. Microbiol. Biotechnol. 14, 203–211.
Vogel, H., Todaro, C., 1997. Fermentation and Biochemical Engineering Handbook. Noyes.
Yu, X.L., 2008. Pharmaceutical quality by design: product and process development, understanding, and control. Pharm. Res. 25, 781–791.
Zhang, H., Lennox, B., 2004. Integrated condition monitoring and control of fed-batch fermentation processes. J. Process Control 14, 41–50, http://www.sciencedirect.com/science/article/pii/S0959152403000441